Covalent linking DNA to graphene oxide and its comparison with physisorbed probes for Hg^{2+} detection

Chang Lu,[1,2] Po-Jung Jimmy Huang,[2] Yibin Ying[1,*] and Juewen Liu[2,*]

1. College of Biosystems Engineering and Food Science, Zhejiang University, Hangzhou 310058, China

Email: ybying@zju.edu.cn

2. Department of Chemistry, Waterloo Institute for Nanotechnology, University of Waterloo, Waterloo, Ontario, Canada, N2L 3G1.

Email: liujw@uwaterloo.ca

Abstract

Graphene oxide (GO) has attracted extensive research interest as a platform for DNA adsorption and biosensor development. While most researchers use simple physisorption of fluorescently labeled DNA, covalent sensors are less susceptible to non-specific probe displacement and minimize false positive results. In this work, three thymine-rich DNA probes of different lengths are modified on their 3′-end with an amino group for covalent conjugation to GO. They also each contain an internally labeled fluorophore so that Hg^{2+} binding can lead to a large distance increase between the fluorophore and the GO surface for fluorescence signaling. Hg^{2+}-dependent fluorescence signaling from the covalent sensors are compared with that from the non-covalent sensors in terms of sensitivity, selectivity, signaling kinetics, and continuous monitoring. The covalent sensors are much more stable and resistant to non-specific probe displacement, while still retaining high sensitivity and similar selectivity. The detection limits are 16.3 and 20.6 nM Hg^{2+}, respectively, for the covalent and non-covalent sensors, and detection of spiked Hg^{2+} in Lake Ontario water is demonstrated.

Keywords: graphene; DNA; mercury; biosensors; fluorescence; covalent

1. Introduction

As a platform for biosensor development, graphene oxide (GO) has attracted extensive interest since its initial report in 2009 (Chen et al. 2012; He et al. 2010; Kuila et al. 2011; Liu et al. 2014b; Lu et al. 2009; Mei and Zhang 2012; Shao et al. 2010). Typically, a fluorescently labeled DNA probe is physisorbed onto the GO surface, resulting in quenched fluorescence. In the presence of a target analyte, which can change the DNA conformation from a single-stranded random coil to a folded structure, the probe DNA is desorbed from the GO surface to enhance fluorescence. Many target analytes have been successfully detected using this method, including complementary nucleic acids, small molecules, proteins and metal ions (Lu et al. 2010; Wang et al. 2010; Wen et al. 2010).

While this physisorption method is effective and simple, the adsorbed DNA probes are susceptible to non-specific displacement, leading to false positive results (Wu et al. 2011). This is particularly a concern if the sensor is to be used in a complex sample matrix. One way to compensate for non-specific displacement is to use an internal standard DNA that is insensitive to the target molecule with a different fluorophore label, and this has been successfully demonstrated for intracellular ATP measurement (Tan et al. 2012). Another method is to covalently link DNA probes (Huang and Liu 2012b; Li et al. 2013; Liu et al. 2014a; Mohanty and Berry 2008; Zhang et al. 2013). While DNA has been covalently attached to many types of surfaces, such as gold nanoparticles (Maxwell et al. 2002; Rosi and Mirkin 2005; Wu et al. 2013), and carbon nanotubes (Jeng et al. 2006), GO has its own advantage of high colloidal stability, easy to handle, and appropriate affinity for DNA adsorption (Liu et al. 2014b).

Mercury is a highly toxic heavy metal, and its detection has been a focus of research in the biosensor field (Kim et al. 2012; Lin et al. 2011; Nolan and Lippard 2008). DNA molecules

are particularly versatile for Hg^{2+} sensing. A number of mechanisms have been developed including thymine-Hg^{2+}-thymine base pairing (Chiang et al. 2008; Dave et al. 2010; Lee et al. 2007; Liu and Tian 2005; Liu and Lu 2007; Ono and Togashi 2004; Wang et al. 2008), Hg^{2+}-activated DNAzymes (Hollenstein et al. 2008; Huang and Liu 2014), and Hg^{2+}-induced cleavage of phosphorothioate RNA (Huang et al. 2015), all showing excellent sensitivity and specificity. Among these, thymine-rich DNA has been most extensively explored. Physisorption of a thymine-rich DNA on GO for Hg^{2+} sensing has already been reported (Cui et al. 2015; He et al. 2010; Huang et al. 2014; Huang et al. 2016; Liu et al. 2011; Zhang et al. 2012). In this work, we test whether covalently linked probes can be used, and how do these two sensors compare in terms of Hg^{2+} detection.

2. Experimental section

2.1. Chemicals

The DNA samples were from Integrated DNA Technologies (Coralville, IA). The FAM- and amino-labeled DNA sequences and modifications are listed in Figure 1C. Carboxyl GO was purchased from ACS Material (Medford, MA). Sodium nitrate, magnesium chloride, 4-morpholineethanesulfonate (MES), tris(hydroxymethyl)aminomethane (Tris) and 4-(2-hydroxyethyl) piperazine-1-ethanesulfonate (HEPES) were from Mandel Scientific (Guelph, Ontario, Canada). Cerium chloride heptahydrate, manganese chloride tetrahydrate, magnesium nitrate, cobalt chloride hexahydrate, copper chloride dihydrate, zinc chloride, cadmium chloride hydrate, mercury perchlorate, lead acetate, sodium chloride, calcium chloride dihydrate, silver nitrate, Tween 80, Triton X-100, bovine serum albumin (BSA), and N-(3-dimethylaminopropyl)-N-ethylcarbodiimide hydrochloride (EDC·HCl) were from Sigma-Aldrich. The solutions were

made by directly dissolving the salts in Milli-Q water. Milli-Q water was used for all the experiments.

2.2. Covalent DNA conjugation

Three kinds of DNA were used for conjugation, as shown in Figure 1. Each reaction was carried out in a glass vial with a final volume of 500 μL containing GO (200 μg/mL), amino-modified probe DNA (4 μM), NaCl (25 mM), EDC·HCl (10 mM, freshly prepared), and MES (25 mM, pH 6.0) at room temperature under magnetic stirring for overnight. Then the solution was purified by centrifugation at 15000 rpm for 10 min followed by removing the supernatant and washing with 500 μL of urea (8 M) twice to further remove non-covalently linked DNA. To further remove non-covalently attached DNA, the samples were washed with 80% isopropanol followed by dispersing the sample in 5 mM pH 9.5 Tris. Sonication was performed occasionally to assist dispersing (30 sec for three times; Bransonic 1510R-MT). This procedure was repeated three times. Then the sample was washed with water. The sample was then dispersed in buffer A (25 mM HEPES, pH 7.5, 150 mM NaCl, 1 mM $MgCl_2$) containing 4 μM cDNA to fully desorb physisorbed DNA probes. Finally, cDNA was washed away using 80% isopropanol followed by 5 mM Tris, pH 9.5 and 8 M urea at 90 °C. Then the sample was washed with water twice. The covalent sensor of probe 1-3 was dispersed in buffer B (25 mM HEPES, pH 8.0, 150 mM $NaNO_3$), and stored at 4 °C with a final GO concentration of 200 μg/mL. These are referred to as solutions I-III.

2.3. Physisorbed sensor preparation

The same DNA probes were used for preparing physisorbed sensors. Adsorption took place for 30 min in dark at room temperature with a volume of 500 μL containing GO (200 μg/mL) and the DNA probes (4 μM) in buffer B. Then the sensors were washed with buffer B by

centrifugation at 15,000 rpm for 10 min for three times. These physisorbed sensors with probes 1-3 were finally dispersed in buffer B, and stored at 4 °C with a final GO concentration of 200 μg/mL. These are referred to as solutions IV-VI.

2.4. Sensor testing

In a typical experiment for cDNA detection, a final of 4 μM cDNA was added to a sensor consist of 45 μL buffer A and 5 μL solution I-VI, followed by measuring the fluorescence of each sensor using a microplate reader (M3, SpectraMax). To study the response of the sensors to Hg^{2+}, 1 μM Hg^{2+} was added to 45 μL buffer B and 5 μL solution I-VI. To acquire fluorescence spectrum of the sensors, probe 3 was used. Buffer B (180 μL) and 20 μL solution III or VI were mixed, and then 1 μM Hg^{2+} was added. The fluorescence spectra were collected using a Varian Eclipse fluorometer. Then the samples were centrifuged and the supernatant fluorescence was measured again. To detect Hg^{2+}, 5 μL of solution I-VI was dispersed in 45 μL buffer B, and then different concentrations of Hg^{2+} were added. The sensing kinetics were followed. Selectivity tests were performed using the same method by replacing Hg^{2+} with other metal ions. To investigate the sensor stability, both sensors using probe 3 was incubated with BSA, tween 80 and triton X-100 (final 0.1% each).

2.5. Gel-based assay

To perform the Gel-based activity assays using probe 3, buffer B (8 μL) and solution III or VI (2 μL) were mixed and 1 μM Hg^{2+} was added. After 1 h, the samples were centrifuged at 15,000 rpm for 10 min, and the supernatant was collected. Another group without centrifugation was also collected. All the samples were separated on 10% dPAGE gels and analyzed using a Bio-Rad ChemiDoc MP imaging system.

2.6. Reversibility test

To analysis the reversible ability of the sensors, 1 μM Hg^{2+} was added into both sensors using probe 3. Then 5 μM KI was added. After the signal stabilizing, 5 μM Hg^{2+}, 10 μM KI, and 5 μM Hg^{2+} was again added sequentially. The procedure was continuous monitored by the M3 microplate reader.

3. Results and discussion

3.1. Sensor design

Since we are interested in covalent sensors, our DNAs were labeled with an amino group at the 3′-end. If we label a fluorophore on the other end, Hg^{2+}-induced DNA folding will bring the fluorophore to the amino group, which is right at the surface. Therefore, it cannot result in a large fluorescence increase. To solve this problem, we employed an internal fluorophore label and a scheme of our design is shown in Figure 1A. The amino-terminus of the DNA is covalently linked to the carboxyl group on the GO surface via EDC coupling. We expect Hg^{2+}-induced DNA hairpin formation, and the fluorophore is at the loop part of the hairpin to enhance fluorescence. A total of three probes were used, binding 4, 7, and 10 Hg^{2+} ions respectively (Figure 1C). These probes can position the fluorophore 5, 9, and 13 base pairs away from GO surface, respectively (if we count the loop sequences, the distance might be even longer). The same DNAs were also tested for physisorption-based sensing (Figure 1B). In this case, Hg^{2+} binding completely desorbs the DNAs and the sensors should produce higher responses. The binding chemistry between thymine and Hg^{2+} is shown in Figure 1D, and this Hg^{2+} mediated T-T base pairing is even larger compared to a normal T-A base pair (Miyake et al. 2006; Tanaka et al. 2007).

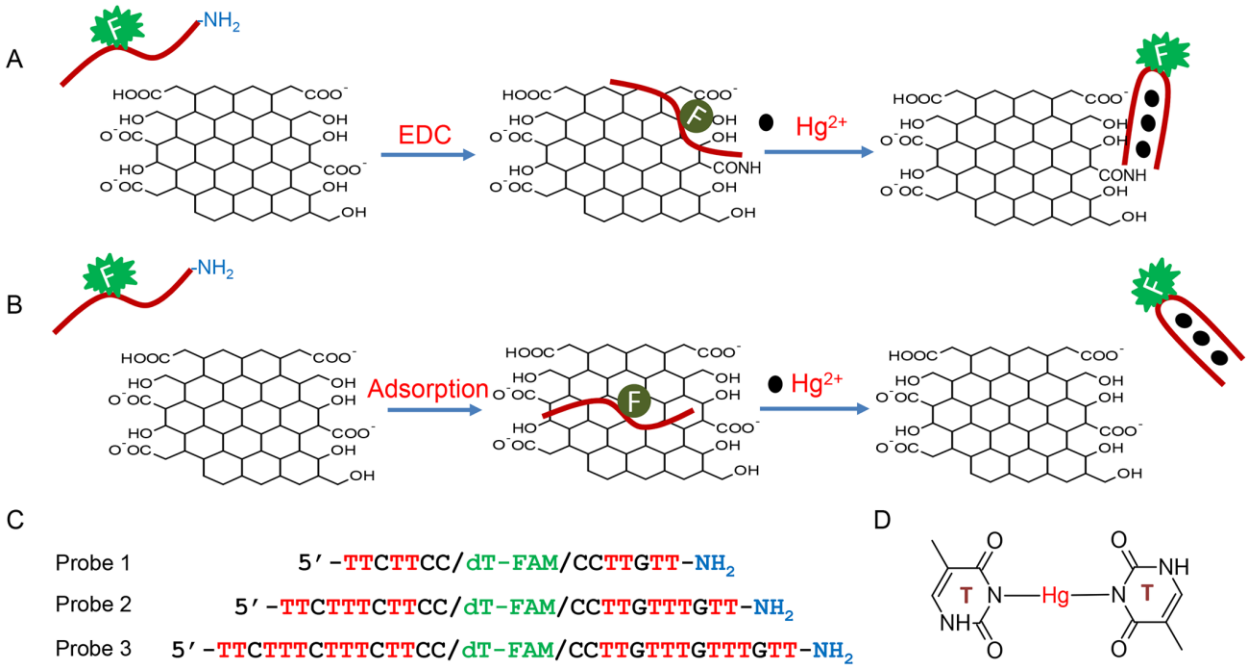

Figure 1. Schematics of preparation and operation of (A) the covalent and (B) the non-covalent sensors. (C) The sequences and modifications of the three DNA probes used in this work. They all contained an amino group and an internal FAM labeled on a thymine base. The Hg^{2+}-binding thymine bases are marked in red. (D) The structure of a Hg^{2+}-mediated thymine base pair.

3.2. Sensor preparation and characterization

GO is rich in carboxyl groups on its edges (Bagri et al. 2010). The size of our GO was determined to be > 2 μm using dynamic light scattering (DLS). We used large GO sheets to facilitate subsequent centrifugation steps. The covalent sensors were prepared using EDC to couple the amino-modified DNAs with the carboxyl on GO to form amide linkages. Since not all the DNA molecules were covalently attached, the physisorbed DNAs need to be removed. Otherwise, they may interfere with data analysis. To achieve this, the samples were extensively

washed using urea, cDNA, and isopropanol (Huang and Liu 2012b; Park et al. 2013). Finally, the coupling efficiency was estimated by reacting 4 μM of the cDNA of probe 3 with the washed covalent sensor. After forming duplex, these immobilized probes were still partially quenched by the GO surface. We previously estimated the quenching efficiency for this probe DNA to be ~90% (Huang and Liu 2012a). After taking this into account and comparing the fluorescence intensity with the same amount of the free DNA before coupling, we obtained a coupling efficiency of ~20%. For preparing physisorbed sensors, the same DNA probes were mixed with GO in buffer B (150 mM $NaNO_3$, HEPES, pH 8). Then the samples were washed using buffer B three times. The physisorbed sensors have an adsorption efficiency of ~67%, and therefore, there are more probes on the physisorbed system.

To confirm that covalent linkages were achieved, we then added the cDNA of the probes to each sensor. For the covalently linked probes, a low background fluorescence was observed for all the sensors (Figure 2A). After adding the cDNAs, fluorescence enhancement was immediately achieved. The longer DNA probes produced higher fluorescence, which is consistent with the increased distance between the internal fluorophore and the surface (Huang and Liu 2012a; Kim et al. 2010). For the non-covalent sample (Figure 2B), all the probes yielded a similar fluorescence increase, which is consistent with the probes leaving the surface. This different DNA length-dependent response between these two types of sensors supports that the covalent sensors were successfully prepared.

It needs to be noted that the final fluorescence intensity is much lower for the covalent sensor (only reached ~20 unit for the probe 3), while the same probe reached ~200 unit for the non-covalent sensor. This can be attributed to the much higher physical adsorption capacity of the non-covalent sensor. Note that only ~20% of the added probes were covalently linked. In

addition, the covalent probes do not leave the surface and the fluorophore is still partially quenched by the surface. Both contributes to the lower overall signal. In terms of the fold of fluorescence intensity change, the covalent sensor still reached about 10-20-fold increase, which is similar to that from the non-covalent sensors.

The kinetics of the response is quite similar for both types of sensors, taking over 2 h to establish a stable fluorescence regardless of the probe length. This might be related to the slow diffusion of the cDNA to the GO surface, and the competition between DNA and GO for probe binding (Liu et al. 2013; Tang et al. 2010). It needs to be noted that most of the signal change occurred within ~20 min, and these sensors still allow relatively fast detection.

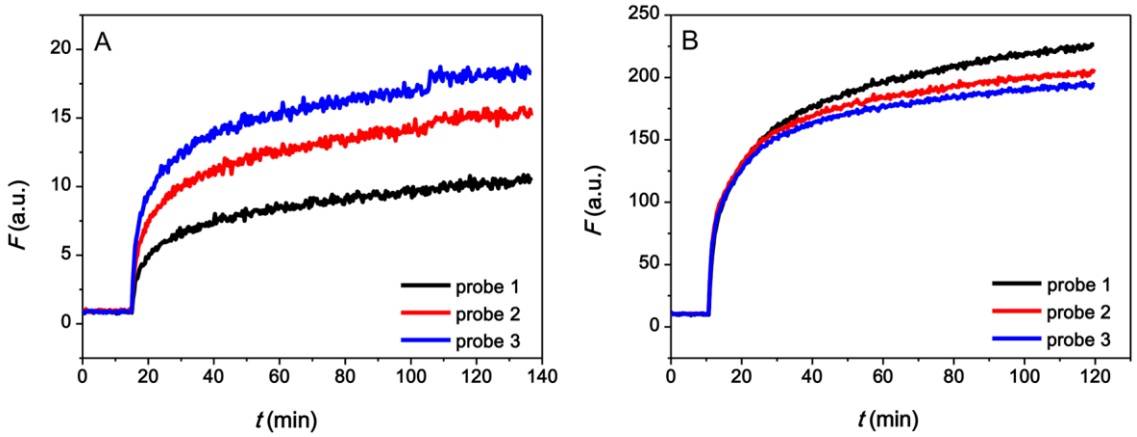

Figure 2. Kinetics of sensor signaling after adding 4 µM cDNA at 10 min to (A) the covalent sensors and (B) the non-covalent sensors. The background signals were monitored for 10-15 min and then the cDNAs were added. Buffer: 150 mM NaCl, 1 mM $MgCl_2$, 25 mM HEPES pH 7.5.

3.3. Sensor response to Hg^{2+}

After confirming the successful covalent conjugation using cDNA, we next tested their responses to Hg^{2+}. Probe 3 was used for this purpose. After adding Hg^{2+}, we centrifuged both samples and

then measured the fluorescence spectra of both the precipitants (re-dispersed), and the supernatants. For the covalent sensor (Figure 3A), the fluorescence of supernatant was low, while the precipitant was more fluorescent. For the non-covalent sensor, the trend inversed (Figure 3B). We also conduct a gel-based assay (Figure 3C). We added Hg^{2+} to the covalent sensor, and the sample was loaded in lane 1. Fluorescence was observed only in the well. We then centrifuged the sample and loaded the supernatant in lane 2, where no fluorescent bands were observed, suggesting that all the DNA was immobilized on GO even after Hg^{2+} treatment. For the non-covalently linked sample, a dark band was observed in lane 3; the supernatant loaded in lane 4 after Hg^{2+} addition also showed a band at the same position, which is the desorbed DNA in the presence of Hg^{2+}. This set of experiments indicated that Hg^{2+} can induce the expected fluorescence response to both sensors.

We next tested all the three DNA probes. After adding Hg^{2+}, we observed a similar response for all the covalent sensors (Figure 3D). This is different from the pattern of the cDNA reaction. The fact that all the three covalent sensors responded similarly to Hg^{2+} suggests that fewer longer probes reacted with Hg^{2+}. This might be due to the higher affinity of the longer DNA with the surface, and thus relatively fewer molecules reacted. For the non-covalent sensors, the shortest probe 1 had the highest fluorescence increase (Figure 3E). This is also consistent with that the shorter DNA is more easily desorbed. Here it is interesting to note that it takes less time for Hg^{2+} to reach a steady fluorescence, while adding cDNA takes much longer time. Hg^{2+} can establish equilibrium faster than the cDNA, possibly due to its smaller size.

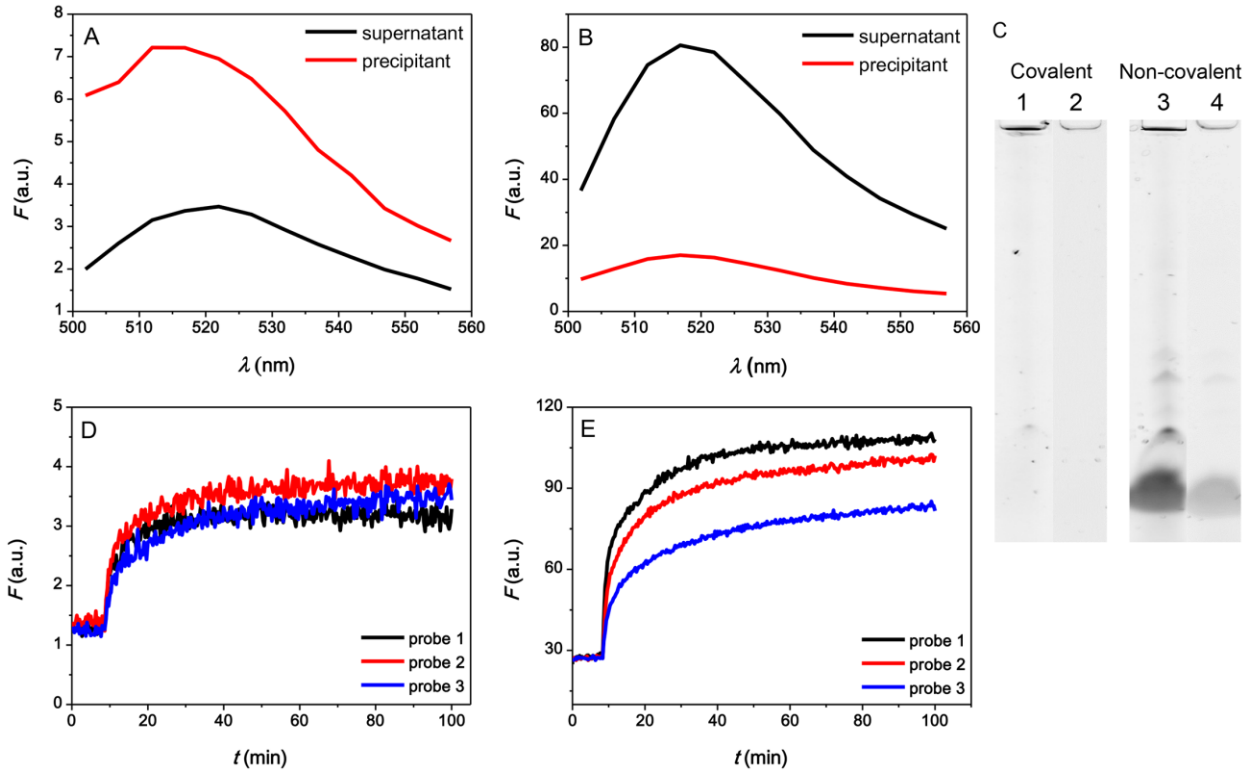

Figure 3. Fluorescence spectra of (A) the covalent and (B) the non-covalent probe 3 sensors after reaction with 1 μM Hg^{2+} and centrifugation. The precipitants were re-dispersed in the same buffer. (C) Gel images of the covalent (lane 1, 2) and noncovalent (lane 3, 4) probe 3 sensors after reaction with 1 μM Hg^{2+} before (lane 1, 3) and after centrifugation (lane 2, 4). Kinetics of fluorescence increase for (D) the covalent and (E) the non-covalent sensors in the presence of 1 μM Hg^{2+} added at 10 min. Buffer: 150 mM $NaNO_3$, 25 mM HEPES, pH 8.0.

3.4. Sensitivity comparison.

Next we measured the sensor response as a function of Hg^{2+} concentration. The kinetics of the covalent and non-covalent sensor responses are shown in Figure 4A, and B, respectively. Both sensors showed Hg^{2+} concentration-dependent fluorescnece enhancement, allowing quantitative measurement. The covalent sensor is more noisy since it has a lower DNA density and thus less

signal. We plotted the fluorescence intensity at 10 min after adding Hg^{2+} for the two types of sensors (Figure 4C, D). The 5F show the linear response at the low Hg^{2+} concentration regions. The detection limits are 16.3 and 20.6 nM Hg^{2+}, respectively, for the covalent and non-covalent sensors. The slope of the calibration curves represent the sensitivity of the sensors. We normalized the fluorescence by their initial intensity before Hg^{2+} addition, and the slopes are 1.58 and 1.93 fold/μM Hg^{2+} for the covalent and non-covalent sensors. Therefore, in terms of detection limits and sensitivity, both sensors are comparable.

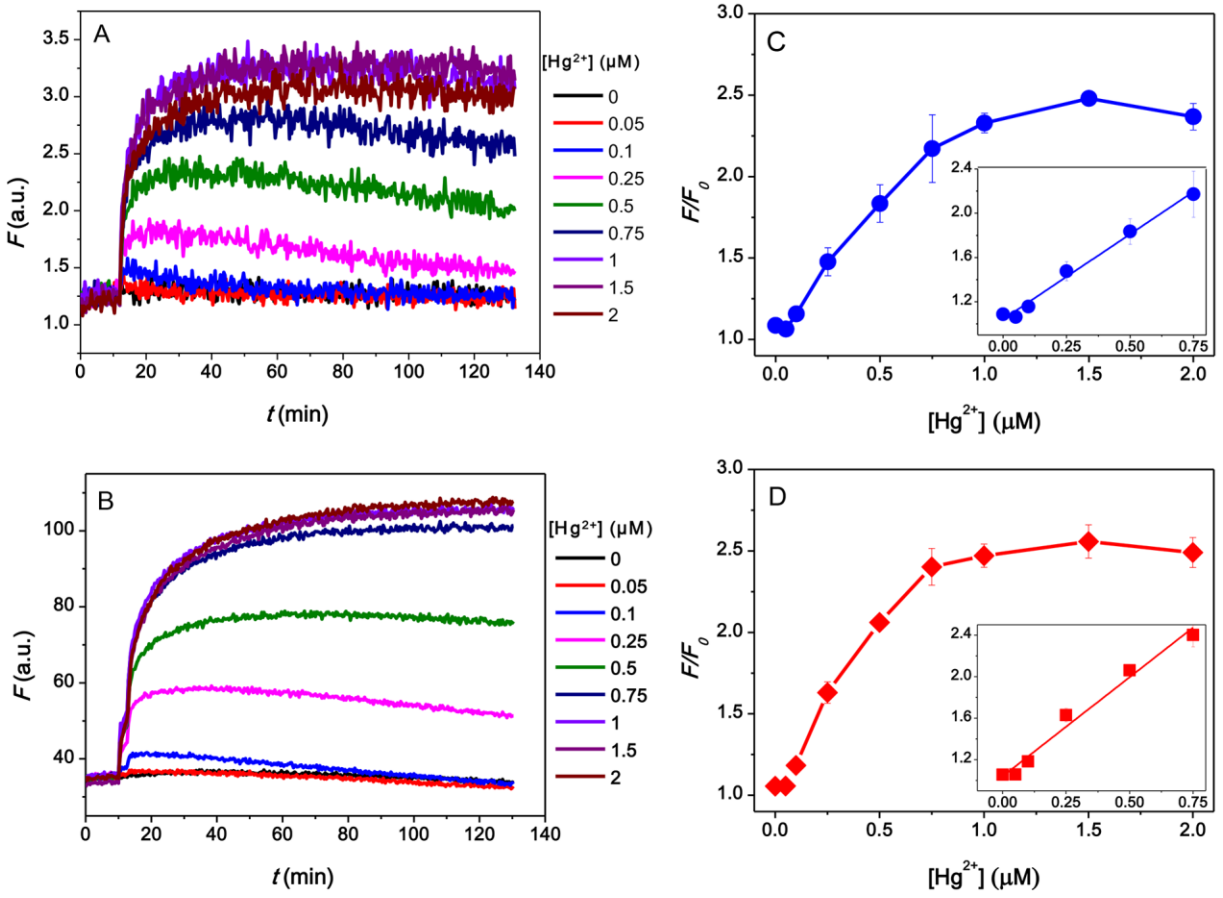

Figure 4. Sensor sensitivity test. Sensor signaling kinetics in the presence of various concentrations of Hg^{2+} for (A) the covalent and (B) the non-covalent probe 1. Sensor response at 10 min after adding Hg^{2+} for (C) the covalent probe 1 with the detection limit of 16.3 nM, and (D)

the non-covalent probe 1 with the detection limit of 20.6 nM. Insets: response at low Hg^{2+} concentrations for calculating the detection limits and sensitivities. *F* presents the final fluorescence and F_0 presents the initial fluorescence. Buffer: 150 mM $NaNO_3$, 25 mM HEPES, pH 8.0.

3.5. Selectivity

After sensitivity, we next compared the selectivity of both type sensors. With 1 μM metal ions, Hg^{2+} yielded the highest response among all the divalent metal ions (Figure 5A). Interestingly, Ag^{+} also produced a significant response, and this is attributed to the relatively high affinity between Ag^{+} and pyrimidine bases (Urata et al. 2011). A similar response was observed with the non-covalent sensor (Figure 5B). Overall, other metal ions did not produce any signal, confirming the high selectivity of the covalent probe is still retained for Hg^{2+}. By reading the literature, most previous work did not test Ag^{+} (Lee et al. 2007; Liu and Lu 2007; Ono and Togashi 2004; Wang and Liu 2008; Wang et al. 2008). Using SYBR Green I staining, we previously showed that Ag^{+} did not interfere with Hg^{2+} detection (Dave et al. 2010; Helwa et al. 2012). Here we also measured the Ag^{+} and Hg^{2+} response with a different DNA using SYBR Green I in Figure S1 (Supplementary data). Therefore, the interference from Ag^{+} might be removed by designing different probe sequences or using other signaling mechanisms (Ono et al. 2008). We further tested the sensors in Lake Ontario water and both type of sensors can detect spiked Hg^{2+} with a similar performance (Figure S2).

3.6. Sensor stability

To test the stability of the sensors against non-specific displacement by non-target molecules, we challenged both type sensors using Tween 80, a common surfactant. With 0.1% Tween 80, the

non-covalent sensor showed a very significant fluorescence enhancement (Figure 5C), suggesting that this sensor is highly susceptible to false positive signal. See Figure S3 for the original data without normalization. On the other hand, the covalent sensor had much less response. Therefore, although both sensors have a similar selectivity profile against various metal ions, the covalent sensor is better at resisting to non-specific probe displacement.

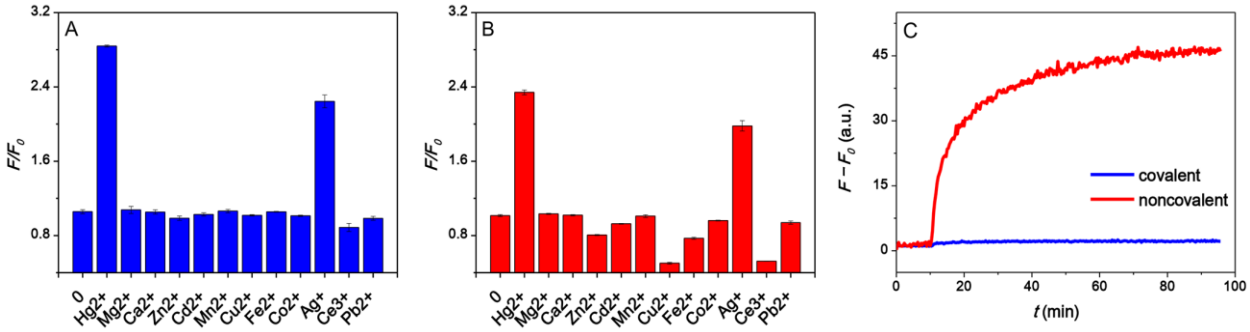

Figure 5. Fluorescence change of (A) the covalent and (B) the non-covalent sensors using probe 3 after adding various metal ions (1 μM each, 90 min reaction time). (C) Response of the covalent and non-covalent sensors with probe 3 to 0.1% Tween 80 added at 10 min. Buffer: 150 mM $NaNO_3$, 25 mM HEPES pH 8.

3.7. Continuous monitoring

For certain applications, it is important to have a reversible sensor response, such as continous monitoring of analyte concentration fluctuation. To test this, we designed the followed experiments to modulate Hg^{2+} concentration by adding iodide. Iodide can strongly bind Hg^{2+} and reduce its free concentration in water. Starting with the clean sensors with a low background fluorescence, we added 1 μM Hg^{2+} to both the covalent and non-covalent sensors prepared with probe 3, and fluorescence enhancement was observed in both. Then 5 μM I^- was added to bind

Hg^{2+} and the DNA was expected to re-adsorb with fluorescence quenched. The covalent sensor has a much faster response in this regard and the signal approached to the initial background level (Figure 6A). The non-covalent senosr dropped only ~50% (Figure 6B), suggesting that the other half of the probe remained in the solution. Under the detection condition, the kinetics for DNA adsorption is slow, but the covalent sensor does not need to diffuse and thus has faster recovery. This process was repeated a few times and the same response pattern was consistently observed. This suggests that the covalent sensor is better than the non-covalent one for monitoring the fluctuation of Hg^{2+} concentration since it has a faster kinetics of getting back to the initial state.

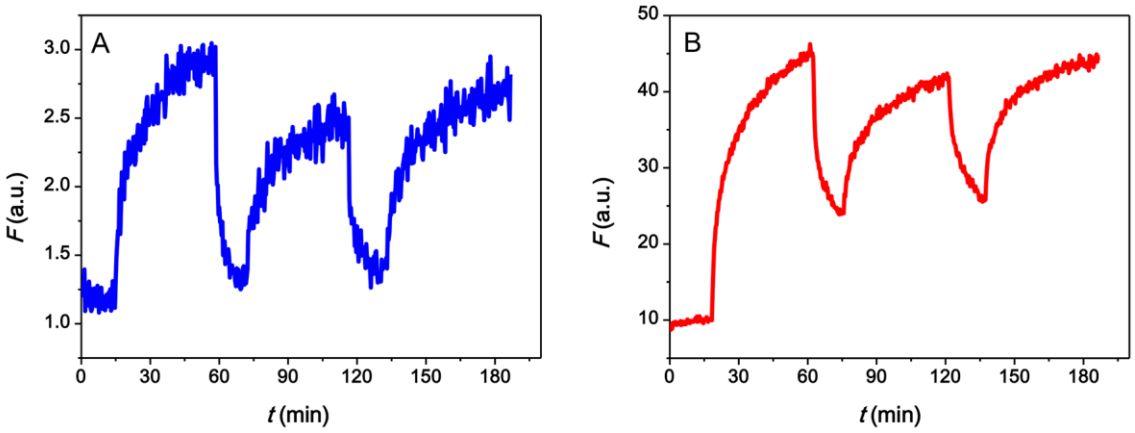

Figure 6. Relative fluorescence signaling of (A) the covalent sensor and (B) the non-covalent sensor for continous monitoring of Hg^{2+} concentration after adding 1 μM Hg^{2+} at 15 min, 5 μM I^- at 60 min, 10 μM Hg^{2+} at 73 min, 5 μM I^- at 117 min and 10 μM Hg^{2+} at 133 min. The dashed lines indicate the background fluorescence intensity. Buffer: 150 mM $NaNO_3$, 25 mM HEPES, pH 8.

4. Conclusions

In summary, we prepared covalent sensors for Hg^{2+} detection based on fluorescent DNA probes of different lengths. The same sequences were also used to prepare physisorbed probes for comparison. The covalent linkages were verified by cDNA test, centrifugation assay, and gel electrophoresis. In the present of Hg^{2+}, fluorescence signaling was achieved for all these sensors in a Hg^{2+}-dependent manner. Both types of sensors have similar sensitivity and selectivity. The covalent sensor allows reversible sensing, while the non-covalent sensor gives higher fluorescence signal at the same GO concentration. The covalent sensor is much more resistent to non-specific probe displacement. This study represents an effort to covalently link DNA to the surface of GO for detecting Hg^{2+} and suggests an important role of covalent sensors in analytical applications.

Acknowledgement

This work is supported by the Natural Sciences and Engineering Research Council of Canada (NSERC). Chang Lu is supported by a Doctoral Fund for Priority Development Project from the Ministry of Education of China (20120101130009).

Appendix A. Supplementary material

Supplementary data associated with this article can be found in the online version at http://dx.doi.org/10.1016/j.bios.

References

1. Bagri, A., Mattevi, C., Acik, M., Chabal, Y.J., Chhowalla, M., Shenoy, V.B., 2010. Nat Chem 2, 581-587.
2. Chen, D., Feng, H., Li, J., 2012. Chem. Rev. 112, 6027-6053.
3. Chiang, C.K., Huang, C.C., Liu, C.W., Chang, H.T., 2008. Anal. Chem. 80, 3716-3721.
4. Cui, X., Zhu, L., Wu, J., Hou, Y., Wang, P., Wang, Z., Yang, M., 2015. Biosens. Bioelectron. 63, 506-512.
5. Dave, N., Huang, P.-J.J., Chan, M.Y., Smith, B.D., Liu, J., 2010. J. Am. Chem. Soc. 132, 12668–12673.
6. He, S.J., Song, B., Li, D., Zhu, C.F., Qi, W.P., Wen, Y.Q., Wang, L.H., Song, S.P., Fang, H.P., Fan, C.H., 2010. Adv. Funct. Mater. 20, 453-459.
7. Helwa, Y., Dave, N., Froidevaux, R., Samadi, A., Liu, J., 2012. ACS Appl. Mater. Inter. 4, 2228-2233.
8. Hollenstein, M., Hipolito, C., Lam, C., Dietrich, D., Perrin, D.M., 2008. Angew. Chem., Int. Ed. 47, 4346 - 4350.
9. Huang, J., Gao, X., Jia, J., Kim, J.-K., Li, Z., 2014. Anal. Chem. 86, 3209-3215.
10. Huang, P.-J.J., Liu, J., 2012a. Small 8, 977-983.
11. Huang, P.-J.J., Liu, J., 2012b. Anal. Chem. 84, 4192-4198.
12. Huang, P.-J.J., Liu, J., 2014. Anal. Chem. 86, 5999-6005.
13. Huang, P.-J.J., van Ballegooie, C., Liu, J., 2016. Analyst. DOI: 10.1039/C5AN02031J.
14. Huang, P.-J.J., Wang, F., Liu, J., 2015. Anal. Chem. 87, 6890–6895.
15. Jeng, E.S., Moll, A.E., Roy, A.C., Gastala, J.B., Strano, M.S., 2006. Nano Lett. 6, 371-375.
16. Kim, H.N., Ren, W.X., Kim, J.S., Yoon, J., 2012. Chem. Soc. Rev. 41, 3210-3244.

17. Kim, J., Cote, L.J., Kim, F., Huang, J., 2010. J. Am. Chem. Soc. 132, 260-267.

18. Kuila, T., Bose, S., Khanra, P., Mishra, A.K., Kim, N.H., Lee, J.H., 2011. Biosens. Bioelectron. 26, 4637-4648.

19. Lee, J.-S., Han, M.S., Mirkin, C.A., 2007. Angew. Chem., Int. Ed. 46, 4093-4096.

20. Li, M., Zhou, X., Ding, W., Guo, S., Wu, N., 2013. Biosens. Bioelectron. 41, 889-893.

21. Lin, Y.W., Huang, C.C., Chang, H.T., 2011. Analyst 136, 863-871.

22. Liu, B., Sun, Z., Zhang, X., Liu, J., 2013. Anal. Chem. 85, 7987-7993.

23. Liu, B., Tian, H., 2005. Chem. Commun., 3156-3158.

24. Liu, J., Lu, Y., 2007. Angew. Chem., Int. Ed. 46, 7587-7590.

25. Liu, X.F., Miao, L.K., Jiang, X., Ma, Y.W., Fan, Q.L., Huang, W., 2011. Chin. J. Chem. 29, 1031-1035.

26. Liu, Z., Chen, S., Liu, B., Wu, J., Zhou, Y., He, L., Ding, J., Liu, J., 2014a. Anal. Chem. 86, 12229-12235.

27. Liu, Z., Liu, B., Ding, J., Liu, J., 2014b. Anal. Bioanal. Chem. 406, 6885-6902.

28. Lu, C.-H., Li, J., Lin, M.-H., Wang, Y.-W., Yang, H.-H., Chen, X., Chen, G.-N., 2010. Angew. Chem., Int. Ed. 49, 8454-8457.

29. Lu, C.H., Yang, H.H., Zhu, C.L., Chen, X., Chen, G.N., 2009. Angew. Chem. Int. Ed. 48, 4785-4787.

30. Maxwell, D.J., Taylor, J.R., Nie, S., 2002. J. Am. Chem. Soc. 124, 9606-9612.

31. Mei, Q., Zhang, Z., 2012. Angew. Chem., Int. Ed. 51, 5602-5606.

32. Miyake, Y., Togashi, H., Tashiro, M., Yamaguchi, H., Oda, S., Kudo, M., Tanaka, Y., Kondo, Y., Sawa, R., Fujimoto, T., Machinami, T., Ono, A., 2006. J. Am. Chem. Soc. 128, 2172.

33. Mohanty, N., Berry, V., 2008. Nano Lett. 8, 4469-4476.

34. Nolan, E.M., Lippard, S.J., 2008. Chem. Rev. 108, 3443-3480.

35. Ono, A., Cao, S., Togashi, H., Tashiro, M., Fujimoto, T., Machinami, T., Oda, S., Miyake, Y., Okamoto, I., Tanaka, Y., 2008. Chem. Commun., 4825-4827.

36. Ono, A., Togashi, H., 2004. Angew. Chem., Int. Ed. 43, 4300-4302.

37. Park, J.S., Na, H.-K., Min, D.-H., Kim, D.-E., 2013. Analyst 138, 1745-1749.

38. Rosi, N.L., Mirkin, C.A., 2005. Chem. Rev. 105, 1547-1562.

39. Shao, Y.Y., Wang, J., Wu, H., Liu, J., Aksay, I.A., Lin, Y.H., 2010. Electroanalysis 22, 1027-1036.

40. Tan, X., Chen, T., Xiong, X., Mao, Y., Zhu, G., Yasun, E., Li, C., Zhu, Z., Tan, W., 2012. Anal. Chem. 84, 8622-8627.

41. Tanaka, Y., Oda, S., Yamaguchi, H., Kondo, Y., Kojima, C., Ono, A., 2007. J. Am. Chem. Soc. 129, 244.

42. Tang, Z.W., Wu, H., Cort, J.R., Buchko, G.W., Zhang, Y.Y., Shao, Y.Y., Aksay, I.A., Liu, J., Lin, Y.H., 2010. Small 6, 1205-1209.

43. Urata, H., Yamaguchi, E., Nakamura, Y., Wada, S.-i., 2011. Chem. Commun. 47, 941-943.

44. Wang, J., Liu, B., 2008. Chem. Commun., 4759-4761.

45. Wang, Y., Li, Z.H., Hu, D.H., Lin, C.T., Li, J.H., Lin, Y.H., 2010. J. Am. Chem. Soc. 132, 9274-9276.

46. Wang, Z., Lee, J.H., Lu, Y., 2008. Chem. Commun., 6005-6007.

47. Wen, Y.Q., Xing, F.F., He, S.J., Song, S.P., Wang, L.H., Long, Y.T., Li, D., Fan, C.H., 2010. Chem. Commun. 46, 2596-2598.

48. Wu, M., Kempaiah, R., Huang, P.-J.J., Maheshwari, V., Liu, J., 2011. Langmuir 27, 2731–2738.

49. Wu, P., Hwang, K., Lan, T., Lu, Y., 2013. J. Am. Chem. Soc. 135, 5254-5257.

50. Zhang, J.R., Huang, W.T., Xie, W.Y., Wen, T., Luo, H.Q., Li, N.B., 2012. Analyst 137, 3300-3305.

51. Zhang, Y., Zhao, H., Wu, Z., Xue, Y., Zhang, X., He, Y., Li, X., Yuan, Z., 2013. Biosens. Bioelectron. 48, 180-187.